Available online at www.sciencedirect.com
SCIENCE DIRECT
Catalysis Today 114 (2006) 263–271
CATALYSIS TODAY
www.elsevier.com/locate/cattod

Dioxomolybdenum(VI) modified mesoporous materials for the catalytic epoxidation of olefins

Sofia M. Bruno, José A. Fernandes, Luísa S. Martins, Isabel S. Gonçalves *, Martyn Pillinger, Paulo Ribeiro-Claro, João Rocha, Anabela A. Valente **

Department of Chemistry, CICECO, University of Aveiro, 3810-193 Aveiro, Portugal

Available online 15 February 2006

Abstract

Organic–inorganic hybrid heterogeneous catalyst systems were synthesized by the reaction of the dioxomolybdenum(VI) complex $MoO_2Cl_2(THF)_2$ with the mesoporous silica MCM-41 functionalized with a pyrazolylpyridine ligand (MCM-41-PP). Two catalysts were prepared, one of which involved the postsynthesis trimethylsilylation of MCM-41-PP to remove the residual surface silanol groups. The model complex MoO_2Cl_2L {L = ethyl[3-(2-pyridyl)-1-pyrazolyl]acetate} was also synthesized. Elemental analysis of the supported mesoporous materials indicated molybdenum loadings of 8.0 wt.% (0.83 mmol g^{-1}) for MCM-41-PP·MoO_2Cl_2 and 7.0 wt.% (0.73 mmol g^{-1}) for silylated MCM-41-PP·MoO_2Cl_2. The supported materials were further characterized by N_2 adsorption, $^{13}C/^{29}Si$ (CP) MAS NMR, IR and Raman spectroscopy. The spectroscopic data are consistent with the successful formation of tethered complexes of the type MoO_2Cl_2(PP), although the materials also contained an excess of dioxomolybdenum(VI) species that were probably not coordinated directly with the surface-bound ligands. The modified materials are active and selective in the epoxidation of cyclooctene at 328 K using *t*-BuOOH (in decane) as the oxidant and no additional solvent. The initial specific reaction rates were about 350 mol mol_{Mo}^{-1} h^{-1} for the modified materials and also the model complex MoO_2Cl_2L. Stability was checked by recycling the solid catalysts several times. Some activity is lost from the first to second runs, but thereafter stabilizes. The catalytic performance of the hybrid materials was further investigated in the oxidation of α-pinene, (*R*)-(+)-limonene, *trans*-2-octene and 1-octene.

Keywords: Chelating ligands; Dioxomolybdenum(VI) complexes; Epoxidation; Mesoporous materials; Molybdenum; Supported catalysts

1. Introduction

Molybdenum(VI) complexes of the type $MoO(O_2)_2L_n$ [1–4], $MoO_2X_2L_n$ [5–16] and (η^5-C_5R_5)MoO_2X [17–20] (X = F, Cl, Br, alkyl; L = mono or bidentate neutral N,O,S-ligand) are good catalysts or catalyst precursors for olefin epoxidation reactions, usually employing *tert*-butyl hydroperoxide (*t*-BuOOH) as the mono-oxygen source. Important properties, such as the solubility of the complex and the Lewis acidity of the metal center, can be fine-tuned by variation of either X or L. Up until recently, Mo^{VI} complexes like these have been mainly used as homogeneous catalysts. However, attention is now being drawn to the synthesis of heterogeneous catalysts based on these complexes [21–33], since these can be easily separated from a reaction mixture and recycled, which is of significant industrial interest. One approach is to use silica supports modified with functional alkoxy silanes [34]. For example, Jia and Thiel modified the ordered mesoporous silica MCM-41 with a pyrazolylpyridine ligand and prepared a covalently anchored complex of the type $MoO(O_2)_2$(L-L) [21,22]. The hybrid system was highly active and truly heterogeneous for liquid-phase epoxidation of cyclooctene with *t*-BuOOH as the oxygen source. Molybdenum(VI) complexes of the type $MoO_2Cl_2(L_1)(L_2)$ have also been immobilized in MCM-41 derivatized with nitrile and bipyridyl ligands [25,26]. Unfortunately, these catalysts proved to be unstable towards molybdenum leaching, which accounted for nearly complete loss of activity in a second reaction cycle. Better results were obtained using 1,4-diazabutadiene ligands covalently linked to the support, although significant catalytic activity was still lost between the first and second runs [27,28]. In the present work, we have studied

* Corresponding author. Tel.: +351 234 378190; fax: +351 234 370084.
** Corresponding author. Tel.: +351 234 378123; fax: +351 234 370084.
E-mail addresses: igoncalves@dq.ua.pt (I.S. Gonçalves), avalente@dq.ua.pt (A.A. Valente).

0920-5861/$ – see front matter © 2006 Elsevier B.V. All rights reserved.
doi:10.1016/j.cattod.2006.01.007

the immobilization of a bis(chloro)dioxomolybdenum(VI) complex in MCM-41 functionalized with a pyrazolylpyridine ligand. The resulting supported materials and also a model complex containing a pyrazolylpyridine ligand were tested as catalysts for the liquid-phase epoxidation of various olefins, using *t*-BuOOH as the oxidant.

2. Experimental

2.1. Characterization methods

Microanalyses for CHN were performed at the ITQB, Oeiras, Portugal (by C. Almeida), and Mo was determined by ICP-AES at the Central Laboratory for Analysis, University of Aveiro (by E. Soares). Powder XRD data were collected on a Philips X'pert diffractometer using Cu Kα radiation filtered by Ni (λ = 1.5418 Å). Nitrogen adsorption–desorption isotherms were measured at 77 K, using an automatic ASAP 2000 adsorption apparatus (measured by Labgran, IPN). Before analysis, pristine calcined MCM-41 was degassed at 573 K and the modified materials at 413 K (to minimize destruction of the functionalities). The BET specific surface area was calculated on the basis of nitrogen adsorption data in the relative pressure range from 0.01 to 0.1. The pore size distributions (PSDs) were obtained from the adsorption branches of the isotherms using the BJH method with the modified Kelvin equation and a correction for the statistical film thickness on the pore walls [35,36]. The statistical film thickness was calculated using the Harkins–Jura equation in the p/p_0 range from 0.1 to 0.95. IR spectra were obtained as KBr pellets using a FTIR Mattson-7000 infrared spectrophotometer. Raman spectra were recorded on a Bruker RFS100/S FT instrument (Nd:YAG laser, 1064 nm excitation, InGaAs detector). Solid-state magic-angle-spinning (MAS) NMR spectra were recorded at 79.49 MHz for ^{29}Si and 125.76 MHz for ^{13}C on Bruker Avance 400/500 spectrometers. ^{29}Si MAS NMR spectra were recorded with 40° pulses, spinning rates of 5.0–5.5 kHz and 60 s recycle delays. ^{29}Si CP MAS NMR spectra were recorded with 5.5 μs ^{1}H 90° pulses, 8 ms contact time with a spinning rate of 5 kHz and 4 s recycle delays. ^{13}C CP MAS NMR spectra were recorded with 3.5 μs ^{1}H 90° pulses and 2 ms contact time with a spinning rate of 7 kHz and 4 s recycle delays.

2.2. Synthesis of starting materials and intermediates

Purely siliceous MCM-41 was synthesized as described previously using $[CH_3(CH_2)_{13}N(CH_3)_3]Br$ as the templating agent [26]. Calcination was carried out at 813 K for 6 h to remove the surfactant template. Powder XRD (2θ/°, *hkl* in parentheses): 2.51 (1 0 0), 4.32 (1 1 0), 4.98 (2 0 0), 6.57 (2 1 0); $a = 2d_{100}/\sqrt{3} = 40.6$ Å. Prior to the grafting experiment, physisorbed water was removed from calcined MCM-41 by heating at 453 K under reduced pressure for 2 h. All other preparations and manipulations were carried out using standard Schlenk techniques under nitrogen. The silylating agent, Me_3SiCl, was obtained from Aldrich and used as received. Solvents were dried by standard procedures (THF, hexane and toluene with Na/benzophenone ketyl; CH_2Cl_2 with CaH_2), distilled under nitrogen and kept over 4 Å molecular sieves. Literature procedures were used to prepare $MoO_2Cl_2(THF)_2$ [28,37], 2-(3-pyrazolyl)pyridine [38], ethyl[3-(2-pyridyl)-1-pyrazolyl]acetate [1], (3-triethoxysilylpropyl)[3-(2-pyridyl)-1-pyrazolyl]acetamide (PP) [22], and MCM-41 grafted with PP [MCM-41-PP (**1**)] [21,22,39] (Chart 1).

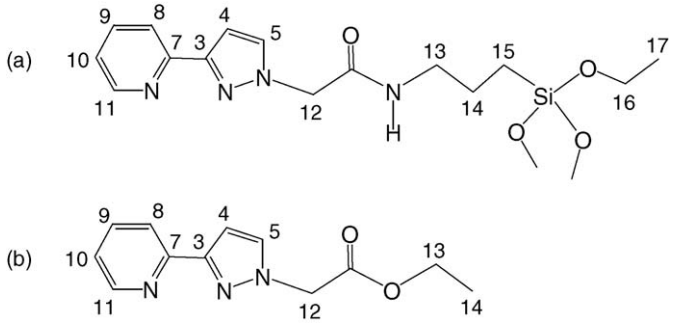

Chart 1. Numbering scheme for the assignment of the NMR spectra of materials **1–4** containing the anchored pyrazolylpyridine ligand (a) and the model complex **5** containing the ligand ethyl[3-(2-pyridyl)-1-pyrazolyl]acetate (b).

2.3. Characterization of MCM-41-PP (*1*)

Elemental analysis found: C, 12.69; H, 1.34; N, 3.16%. IR (KBr, cm^{-1}): 2985 (w), 2938 (w), 1569 (w), 1498 (w), 1457 (w), 1436 (w), 1384 (m), 1363 (w), 1232 (sh), 1082 (vs), 962 (m), 796 (m), 668 (vw), 576 (sh), 458 (vs). Raman (cm^{-1}): 3147 (w), 3130 (w), 3067 (w), 2980 (w), 2936 (m), 2897 (w), 1603 (s), 1573 (m), 1528 (vs), 1497 (w), 1446 (w), 1406 (m), 1364 (w), 1285 (w), 1240 (w), 1154 (w), 1095 (w), 1054 (w), 1008 (m), 964 (m), 796 (w), 709 (w), 630 (w). ^{13}C CP MAS NMR: δ = 167.9 (C=O), 150.3, 147.6 (C^3, C^7, C^{11}), 133.8 (C^5, C^9), 122.9, 120.8 (C^8, C^{10}), 104.9 (C^4), 57.3 (C^{16}), 54.2 (C^{12}), 42.0 (C^{13}), 21.8 (C^{14}), 16.0 (C^{17}), 8.8 (C^{15}) ppm. ^{29}Si MAS NMR: $\delta = -109.4$ (Q^4) ppm. ^{29}Si CP MAS NMR: $\delta = -54.0$ (T^1), -58.8 (T^2), -102.2 (Q^3), -109.8 (Q^4) ppm.

2.4. MCM-41-PP·MoO_2Cl_2 (*2*)

MoO_2Cl_2 (0.30 g, 1.51 mmol) was dissolved in THF (15 mL) and the solution stirred for 20 min at 323 K under nitrogen. The solution was evaporated to dryness and the resultant $MoO_2Cl_2(THF)_2$ dissolved in CH_2Cl_2 (10 mL). This solution was filtered and added to a suspension of MCM-41-PP (**1**) (1.00 g) in CH_2Cl_2 (10 mL) and the mixture stirred at room temperature overnight, under nitrogen. The green solid product was isolated by filtration, washed with CH_2Cl_2 (3 × 15 mL) and dried under reduced pressure for 3 h. Elemental analysis found: C, 10.16; H, 1.19; N, 2.52; Mo, 8.0%. IR (KBr, cm^{-1}): 2994 (w), 1550 (w), 1508 (w), 1490 (w), 1443 (w), 1384 (m), 1236 (sh), 1082 (vs), 951 (m), 916 (m), 882 (w), 796 (m), 687 (w), 618 (w), 564 (m), 459 (s). Raman (cm^{-1}): 1616 (w), 1574 (w), 1534 (w), 1026 (w), 950 (w). ^{13}C CP MAS NMR: δ = 167.1 (C=O), 149.4 (C^3, C^7, C^{11}), 139.0 (C^5, C^9), 124.1 (C^8, C^{10}), 105.5 (C^4), 68.2 (THF), 59.5 (C^{16}), 54.0 (C^{12}), 42.7 (C^{13}), 24.9

(THF), 21.7 (C^{14}), 15.8 (C^{17}), 9.3 (C^{15}) ppm. ^{29}Si MAS NMR: $\delta = -108.3$ (Q^4) ppm. ^{29}Si CP MAS NMR: $\delta = -57.3$ (T^2), -107.9 (Q^4) ppm.

2.5. Silylated MCM-41-PP (3)

Me_3SiCl (5 mL) was added under nitrogen to a suspension of MCM-41-PP (**1**) (1.50 g) in toluene (20 mL) and the mixture stirred at room temperature overnight. The pale yellow solid product was isolated by filtration, washed with CH_2Cl_2 (3×15 mL) and dried under reduced pressure for 3 h at 373 K. Elemental analysis found: C, 13.56; H, 1.77; N, 2.79%. IR (KBr, cm^{-1}): 2938 (w), 1550 (w), 1508 (w), 1465 (w), 1441 (w), 1384 (m), 1235 (sh), 1085 (vs), 961 (w), 848 (w), 795 (m), 668 (w), 563 (sh), 458 (s). Raman (cm^{-1}): 2961 (w), 2932 (w), 2903 (s), 1627 (m), 1602 (m), 1527 (s), 1417 (s), 1003 (m), 963 (m). ^{13}C CP MAS NMR: δ = 168.2 (C=O), 145.6 (C^3, C^7, C^{11}), 133.0 (C^5, C^9), 122.2 (C^8, C^{10}), 105.8 (C^4), 58.9 (C^{16}), 55.1 (C^{12}), 41.8 (C^{13}), 22.3 (C^{14}), 16.6 (C^{17}), 9.4 (C^{15}), −0.9 (Me_3SiO–) ppm. ^{29}Si MAS NMR: δ = 14.7 (Me_3SiO–), −109.3 (Q^4) ppm. ^{29}Si CP MAS NMR: δ = 14.1 (Me_3SiO–), −59.7 (T^2), −65.3 (T^3), −103.3 (Q^3), −108.8 (Q^4) ppm.

2.6. Silylated MCM-41-PP·MoO_2Cl_2 (4)

MoO_2Cl_2 (0.47 g, 2.36 mmol) was dissolved in THF (15 mL) and the solution stirred for 20 min at 323 K under nitrogen. The solution was evaporated to dryness and the resultant $MoO_2Cl_2(THF)_2$ dissolved in CH_2Cl_2 (15 mL). This solution was filtered and added to a suspension of silylated MCM-41-PP (**3**) (1.00 g) in CH_2Cl_2 (10 mL) and the mixture stirred at room temperature overnight, under nitrogen. The solid product was isolated by filtration, washed with CH_2Cl_2 (4×15 mL) and dried under reduced pressure for 3 h at 323 K. Elemental analysis found: C, 11.55; H, 1.56; N, 2.46; Mo, 7.0%. IR (KBr, cm^{-1}): 2960 (w), 1549 (m), 1508 (w), 1484 (w), 1460 (w) 1443 (w), 1384 (m), 1237 (sh), 1081 (vs), 953 (m), 916 (m), 848 (m), 799 (m), 689 (w), 620 (w), 566 (w), 457 (s). Raman (cm^{-1}): 2909 (w), 1616 (w), 1572 (w), 1536 (w). ^{13}C CP MAS NMR: δ = 169.0 (C=O), 149.0 (C^3, C^7, C^{11}), 138.5 (C^5, C^9), 124.0 (C^8, C^{10}), 105.4 (C^4), 67.7 (THF), 59.3 (C^{16}), 53.9 (C^{12}), 42.3 (C^{13}), 25.1 (THF), 21.5 (C^{14}), 16.9 (C^{17}), 9.6 (C^{15}), −0.1 (Me_3SiO–) ppm. ^{29}Si MAS NMR: δ = 14.2 (Me_3SiO–), −108.8 (Q^4) ppm. ^{29}Si CP MAS NMR: δ = 14.4 (Me_3SiO–), −58.7 (T^2), –67.6 (T^3), −108.7 (Q^4) ppm.

2.7. MoO_2Cl_2{ethyl[3-(2-pyridyl)-1-pyrazolyl]acetate} (5)

MoO_2Cl_2 (0.34 g, 1.73 mmol) was dissolved in THF (20 mL) and the solution stirred for 20 min at 323 K under nitrogen. The solution was evaporated to dryness and the resultant $MoO_2Cl_2(THF)_2$ dissolved in CH_2Cl_2 (20 mL). Ethyl[3-(2-pyridyl)-1-pyrazolyl]acetate (0.40 g, 1.73 mmol) was then added and the mixture stirred at room temperature overnight. The solution was evaporated to dryness and the resulting green solid washed with hexane (4×15 mL) and dried under reduced pressure for 3 h (0.71 g, 95%). Anal. calcd for $C_{12}H_{13}Cl_2MoN_3O_4$ (430.09): C, 33.51; H, 3.05; N, 9.77%. Found: C, 33.65; H, 3.05; N, 9.65%. IR (KBr, cm^{-1}): 3144 (m), 3117 (m), 3001 (m), 2953 (w), 1743 (vs), 1613 (s), 1607 (s), 1569 (m), 1535 (w), 1508 (m), 1464 (m), 1438 (s), 1425 (s), 1384 (m), 1373 (s), 1344 (s), 1272 (s), 1242 (s), 1159 (m), 1140 (m), 1098 (s), 1079 (s), 1057 (m), 1024 (s), 964 (m), 938 (vs), 907 (vs), 863 (w), 795 (w), 775 (vs), 747 (m), 710 (m), 693 (m), 645 (m), 560 (m), 503 (m), 436 (w), 426 (m), 401 (m), 384 (w), 364 (w), 341 (s), 313 (w). Raman (cm^{-1}): 3134 (m), 3121 (m), 3071 (m), 2961 (m), 2940 (m), 1610 (m), 1569 (m), 1532 (s), 1427 (w), 1374 (w), 1337 (w), 1291 (w), 1252 (w), 1053 (w), 1037 (w), 1021 (m), 964 (w), 938 (vs), 915 (m), 871 (w). ^{1}H NMR (300.13 MHz, 298 K, $CDCl_3$): δ = 9.41 (d, 1H, H^{11}), 8.07 (t, 1H, H^9), 7.88 (d, 1H, H^8), 7.82 (d, 1H, H^5), 7.62 (t, 1H, H^{10}), 6.97 (d, 1H, H^4), 5.64 (s, 2H, H^{12}), 4.28 (q, 2H, H^{13}), 1.32 (t, 3H, H^{14}) ppm.

2.8. Catalysis

The liquid-phase catalytic oxidations were carried out at 238 K under air (atmospheric pressure) in a reaction vessel equipped with a magnetic stirrer and immersed in a thermostated oil bath. A 1% molar ratio of free complex/substrate (or 175 mg MCM-41-supported catalyst plus 7.2 mmol cyclooctene) and a substrate/oxidant molar ratio of 0.65 (*t*-BuOOH, 5.5 M in decane) were used. The course of the reaction was monitored using a gas chromatograph (Varian 3800) equipped with a capillary column (SPB-5, 20 m × 0.25 mm) and a flame ionization detector. The products were identified by gas chromatography–mass spectrometry (HP 5890 Series II GC; HP 5970 Series Mass Selective Detector) using He as carrier gas.

3. Results and discussion

3.1. Synthesis and characterization

MCM-41 functionalized with a pyrazolylpyridine ligand [MCM-41-PP (**1**)] was prepared as described previously [21,22,39]. Postsynthetic silylation using Me_3SiCl was carried out to remove the residual Si–OH groups on the surface of the mesoporous material, which could be unfavorable for the catalytic reaction (Scheme 1). Trimethylsilylation may have other advantages, such as making the surface more hydrophobic and improving stability against moisture and mechanical compression. The success of the post-synthesis treatment was confirmed by MAS NMR (described below) and IR spectroscopy. Thus, the IR spectrum of compound **1** contains a medium intensity absorption at 962 cm^{-1} which is assigned to the Si–$O^{\delta-}$ of a Si–OH stretch [40]. The relative intensity of this band is already reduced compared with unmodified MCM-41, due to partial derivatization of surface silanol groups. A further reduction to weak intensity was observed upon trimethylsilylation. The presence of Me_3Si groups in silylated MCM-41-PP (**3**) was confirmed by an IR band at 848 cm^{-1}, which is assigned to CH_3 rocking [41]. Dioxomolybdenum(VI) modified materials were subsequently prepared by treatment of

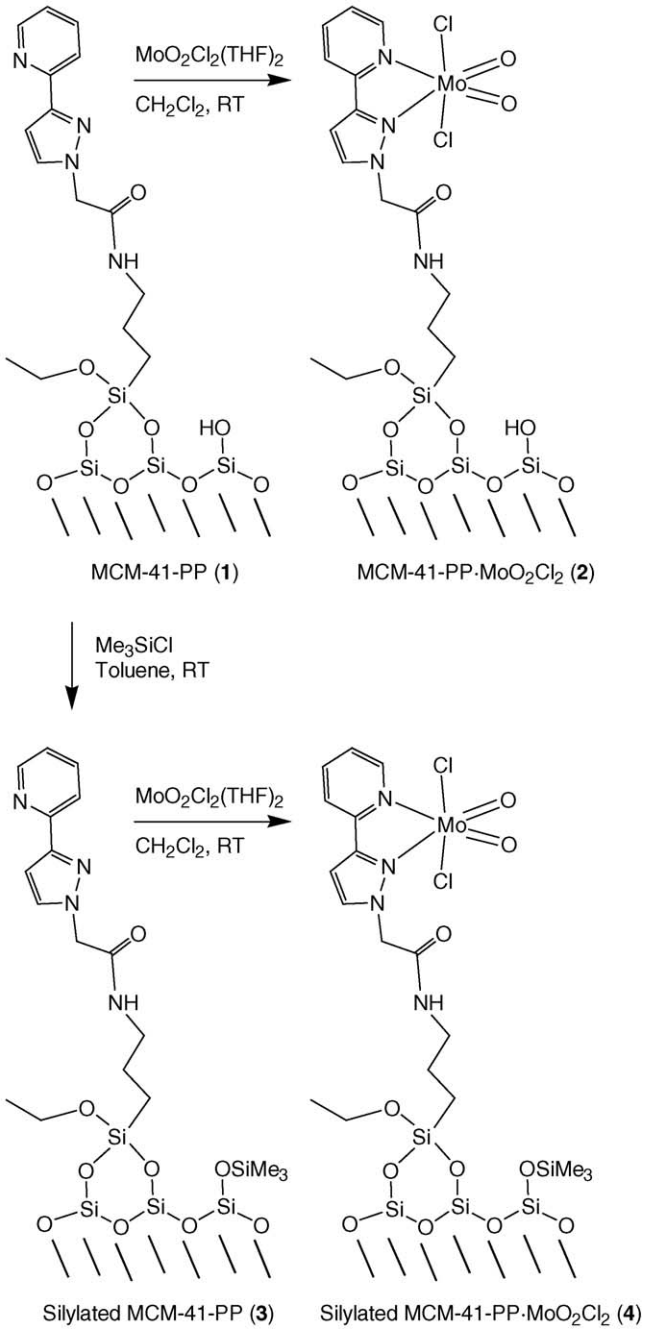

Scheme 1.

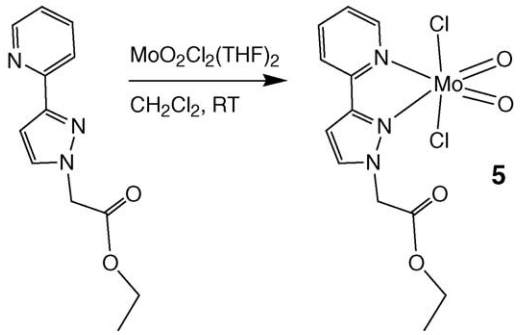

Scheme 2.

1 and **3** with a solution of the complex $MoO_2Cl_2(THF)_2$ in CH_2Cl_2 at room temperature. Elemental analysis indicated metal loadings of 8.0 wt.% (0.83 mmol g^{-1}) for MCM-41-PP·MoO_2Cl_2 (**2**) and 7.0 wt.% (0.73 mmol g^{-1}) for silylated MCM-41-PP·MoO_2Cl_2 (**4**), with ligand contents of about 0.45 mmol g^{-1}. Considering the relatively high metal loadings, it is evident that a certain fraction of Mo centers are not coordinated directly to the surface-bound ligands. One possibility, at least for compound **2**, is that grafted complexes such as $\{MoO_2[(-O)_3SiO]X(THF)_n\}$ were formed (in addition to complexes bearing the surface-bound PP ligand) via direct reaction of the complex $MoO_2Cl_2(THF)_2$ with residual surface silanols [40]. A second possibility is the formation of oxybridged bimetallic species [26]. The model dioxomolybdenum(VI) complex **5**, containing the ligand ethyl[3-(2-pyridyl)-1-pyrazolyl]acetate, was synthesized to provide spectroscopic and catalytic data for comparison with the supported mesoporous materials (Scheme 2).

Like the pristine calcined MCM-41 precursor, the materials **1**–**4** exhibited type IV N_2 adsorption–desorption isotherms (not shown), typical of mesoporous solids (pore width between 2 and 50 nm, according to IUPAC) [42], indicating the preservation of the mesoporous system during the surface modifications. The isotherms exhibited an increase in the amount adsorbed at pressures close to the saturation vapor pressure, which may be due to adsorption on the external surface via multilayer adsorption and/or capillary condensation in inter-particle pores. The step corresponding to capillary condensation in the primary mesopores appeared in the relative pressure range 0.2–0.3 for unmodified MCM-41 and below 0.25 for the modified samples. No appreciable adsorption–desorption hysteresis related to capillary condensation in the primary mesopores was observed, although the samples exhibited desorption irreversibility at relative pressures above about 0.35. The hysteresis behavior observed is typical for nitrogen adsorption at 77 K, where adsorption–desorption hysteresis is usually not observed below a relative pressure of 0.4 [43]. The values of specific surface area (S_{BET}) and total pore volume (V_p) of the unmodified MCM sample used in the present study were 1096 $m^2\ g^{-1}$ and 1.7 $cm^3\ g^{-1}$, respectively (Table 1). The isotherms of the functionalized MCM samples show a lower N_2 uptake, and S_{BET} decreased by 37–50% and V_p decreased by 56–68%. These results are consistent with immobilization of the bulky complexes in the channels of the host. The presence of metal-organic moieties inside the channels was also supported by the decrease of the p/p_0 coordinate of the inflection point of the isotherms upon post-synthesis treatments [44]. Furthermore, the maximum of the PSD curve determined by the BJH method decreased from 3.4 nm for MCM-41 to 2.8 for MCM-41-PP·MoO_2Cl_2 (**2**) and 2.6 nm for silylated MCM-41-PP·MoO_2Cl_2 (**4**).

The ^{13}C CP MAS NMR spectrum of MCM-41-PP (**1**) was assigned as described previously [22,39]. The resonances for the CO and pyrazolylpyridine ring carbon atoms appear in the range δ = 100–170 ppm, and the methylene and methyl groups

Table 1
Texture parameters of MCM samples taken from nitrogen adsorption data

Sample	S_{BET} [$m^2\ g^{-1}$]	ΔS_{BET} (%)[a]	V_P [$cm^3\ g^{-1}$]	ΔV_P (%)[a]	d_p [nm][b]
MCM-41	1096	–	1.7	–	3.4
1	635	42	0.68	60	2.9
2	576	47	0.58	66	2.8
3	686	37	0.74	56	2.6
4	547	50	0.54	68	2.6

[a] Variation of surface area and total pore volume in relation to parent MCM material.
[b] Determined by the BJH method.

present signals between $\delta = 8$ and 60 ppm (Fig. 1). There are residual ethoxy groups, as evidenced by the peaks at about 16 and 57 ppm. Silylated MCM-41-PP (**3**) exhibits an additional peak at $\delta = -0.9$ ppm for the surface $(-O)_3Si-O-SiMe_3$ species. The ^{29}Si MAS and CP MAS NMR spectra of the modified materials **1** and **3** provided direct evidence for the incorporation of the covalently anchored organic systems. Unmodified MCM-41 displays two broad convoluted resonances in the ^{29}Si CP MAS NMR spectrum at $\delta = -111$ and -101 ppm, assigned to Q^4 and Q^3 species of the silica framework, respectively $[Q^n = \underline{Si}(OSi)_n(OH)_{4-n}]$. A weak shoulder is also observed at $\delta = -91$ ppm for the Q^2 species. The Q^3 sites are associated with the single silanols Si–OH (including hydrogen-bonded silanols), and the Q^2 sites correspond to the geminal silanols. Grafting of (3-triethoxysilylpropyl)[3-(2-pyridyl)-1-pyrazolyl]acetamide (PP) (followed by Me_3SiCl, in the case of **3**) into MCM-41 results in a reduction of the Q^3 and Q^2 resonances, and a concomitant increase of the Q^4 resonance (Fig. 2). This is consistent with esterification of the isolated silanol groups by nucleophilic substitution at the silicon atom in the organic compounds. The ^{29}Si CP MAS NMR spectra of **1** and **3** also display a broad peak centered at about $\delta = -59$ ppm, assigned to overlapping resonances for T^1 (δ ca. -54 ppm), T^2 (δ ca. -59 ppm) and T^3 (δ ca. -65 ppm) organosilica species $[T^n = R\underline{Si}(OSi)_m(OEt)_{3-m}]$. A peak at about $\delta = 14.1$ for **3** is assigned to the silicon nuclei of Me_3Si

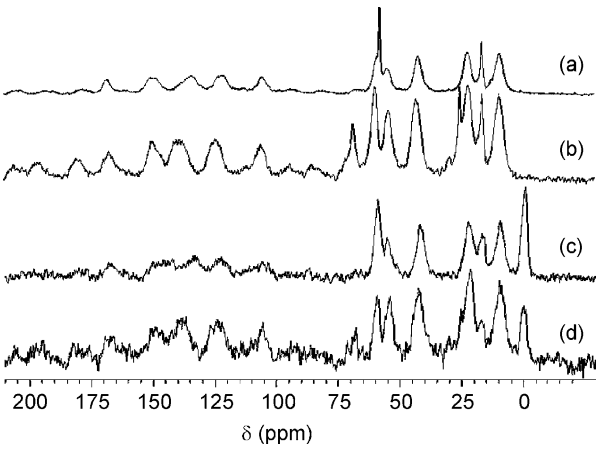

Fig. 1. ^{13}C CP MAS NMR spectra of: (a) MCM-41-PP (**1**), (b) MCM-41-PP·MoO_2Cl_2 (**2**), (c) silylated MCM-41-PP (**3**) and (d) silylated MCM-41-PP·MoO_2Cl_2 (**4**).

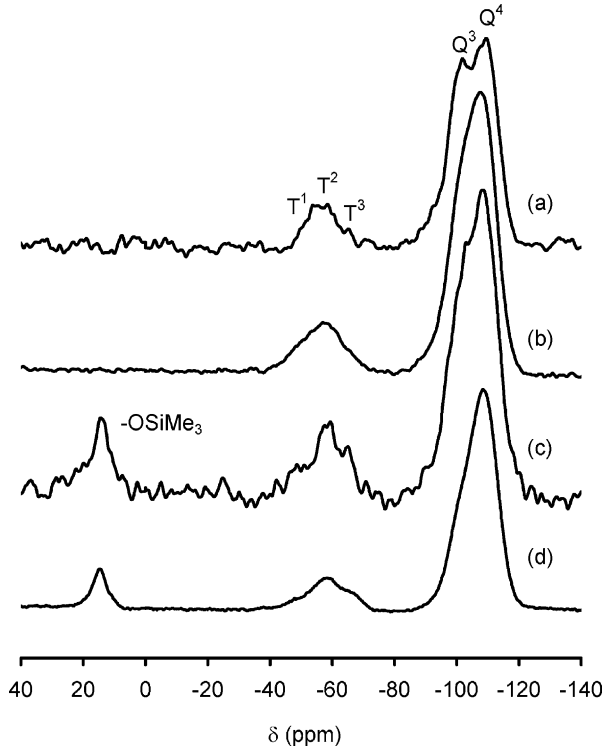

Fig. 2. ^{29}Si CP MAS NMR spectra of: (a) MCM-41-PP (**1**), (b) MCM-41-PP·MoO_2Cl_2 (**2**), (c) silylated MCM-41-PP (**3**) and (d) silylated MCM-41-PP·MoO_2Cl_2 (**4**).

groups. Reaction of the ligand-silicas **1** and **3** with the complex $MoO_2Cl_2(THF)_2$ did not result in significant changes to the ^{29}Si MAS and CP MAS NMR spectra (Fig. 2). However, changes were observed in the ^{13}C CP MAS NMR spectra, in particular concerning the resonances of the pyrazolylpyridine ring carbon atoms (Fig. 1). Thus, the signals for $C^{5/9}$ and $C^{8/10}$ shift noticeably downfield (by up to 8 ppm) after incorporation of the molybdenum complex. On the other hand, the peaks for C^4 and $C^{3,7,11}$ are essentially unaffected. These changes are exactly in line with those reported for the reaction of the complex $MoO(O_2)_2\cdot(DMF)_2$ with the ligand PP, forming the complex $MoO(O_2)_2\cdot$PP in which it was proposed bidentate coordination of the pyrazolylpyridine ligand to the metal center [22].

The IR spectra of MCM-41-PP·MoO_2Cl_2 (**2**) and silylated MCM-41-PP·MoO_2Cl_2 (**4**) support the presence of *cis*-MoO_2 units. Thus, two peaks are observed at about 950 and 916 cm^{-1}. The first peak is attributed to a symmetric Mo=O stretching vibration (overlapping with $Si-O^{\delta-}$ of a Si–OH stretch) and the second peak is assigned to the asymmetric Mo=O stretching vibration. In the model complex **5**, the Mo=O absorptions are more intense and are found at 938 and 907 cm^{-1}. Fig. 3 shows the Raman spectra of the free ligand ethyl[3-(2-pyridyl)-1-pyrazolyl]acetate and the corresponding molybdenum complex **5**. A strong modification of the general profile of the spectrum is observed upon complexation, which is in agreement with the change of the ligand structure and complexation [39]. The most relevant changes are those in the 900–950 cm^{-1} and 1500–1650 cm^{-1} regions. In the first region, the two new bands at 915

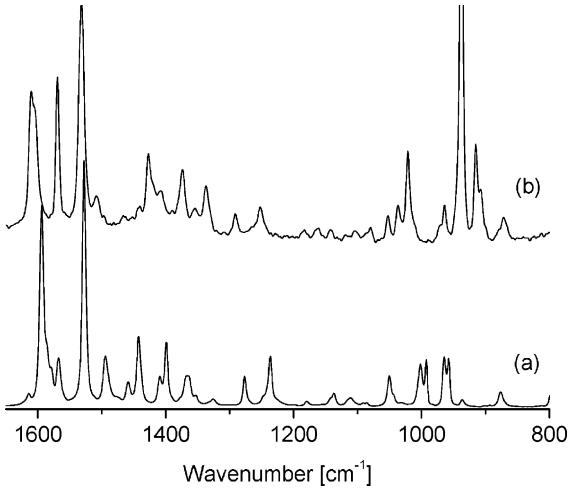

Fig. 3. Selected region of the Raman spectra of the free ligand ethyl[3-(2-pyridyl)-1-pyrazolyl]acetate (a) and the corresponding dioxomolybdenum(VI) complex **5** (b).

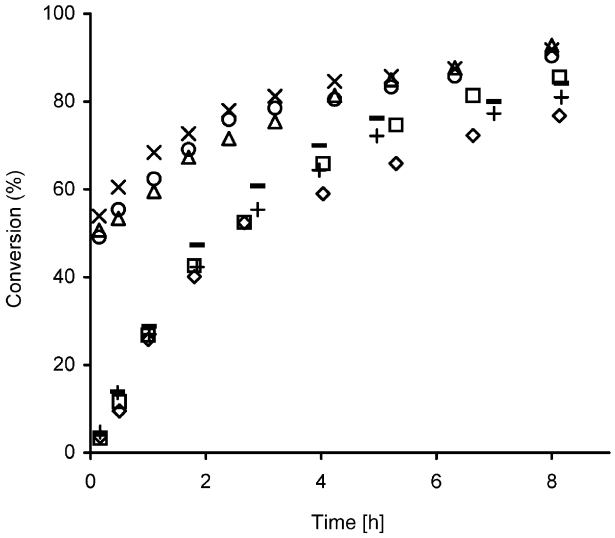

Fig. 4. Kinetic profiles of cyclooctene oxidation with *t*-BuOOH in the presence of complex **5** (×), MCM-41-PP·MoO_2Cl_2 (**2**) [run 1 (○); run 2 (−); run 3 (□)] and silylated MCM-41-PP·MoO_2Cl_2 (**4**) [run 1 (Δ); run 2 (+); run 3 (◇)].

and 938 cm^{-1} are assigned to the MoO_2 asymmetric and symmetric stretching modes, respectively. In the second region, the complexation produces an important intensity change in a group of bands assigned to the ligand modes, yielding a pattern of three intense bands (at 1532, 1569 and 1610 cm^{-1}), which are characteristic of the complex. The Raman spectra of compounds **1**–**4** are dominated by the MCM background, showing a few weak features belonging to the anchored species. For MCM-41-PP (**1**) and silylated MCM-41-PP (**3**), the spectra in the region 1520–1605 cm^{-1} are comparable with that for the free ligand ethyl[3-(2-pyridyl)-1-pyrazolyl]acetate, showing two main bands at 1528 and 1603 cm^{-1}. On the other hand, for compounds **2** and **4**, three sharp bands are observed around 1534–1536, 1572–1574 and 1616 cm^{-1}, which match the general profile and positions of the characteristic bands observed for the model compound **5**. These results are therefore consistent with the formation of a supported complex of the type MoO_2Cl_2(PP) in the materials **2** and **4** (Scheme 1).

3.2. Catalysis

The supported materials **2**, **4** and the model complex **5** were tested as catalysts for the liquid phase epoxidation of cyclooctene using *t*-BuOOH (5.5 M in decane), at 328 K, without additional solvent. No reaction occurs without catalyst or in the presence of pristine calcined MCM-41, suggesting that the molybdenum species are responsible for the catalytic reactions. All catalysts yield epoxycyclooctane as the only product throughout 8 h of reaction. The kinetic profiles of the three catalysts are very similar (Fig. 4), suggesting that the reaction mechanism is similar for the model (**5**) and heterogenized complexes. Initially, the reaction is fast but then slows down somewhat as the reaction proceeds, achieving 100% conversion before 24 h. This behavior is typical of dioxomolybdenum(VI) complexes of the type $MoO_2X_2L_n$ and has generally been attributed to the competition between the substrate and *tert*-butanol, a by-product of the decomposition of *t*-BuOOH, for the coordination to the metal center [14]. The kinetic profiles are all practically coincident and the specific initial reaction rates are of the same order of magnitude (calculated at 10 min and expressed as mol mol_{Mo}^{-1} h^{-1}): **2** (321) < **5** (360) < **4** (379). The specific initial rate observed for the free complex **5** is higher than that of several other dioxomolybdenum(VI) complexes previously studied as catalysts for cyclooctene epoxidation, under similar reaction conditions. Thus, for complexes of the type MoO_2Cl_2[RN = C(R′)-C(R′) = NR] bearing 1,4-R_2-diazabutadiene ligands, TOF (calculated at 1 h) = 14–58 mol mol_{Mo}^{-1} h^{-1} [R = $(CH_2)_2CH_3$, $(CH_2)_3Si(OEt)_3$; R′ = Ph] [27,28] and 179 mol mol_{Mo}^{-1} h^{-1} (R = *p*-tolyl; R′ = CH_3) [13]. For MoO_2Cl_2(4,4′-dimethyl-2,2′-bipyridine), TOF (15 min) = 36 mol mol_{Mo}^{-1} h^{-1} [26], and for [(η^5-C_5H_5)MoO_2Cl], TOF (18 min) = 140 mol mol_{Mo}^{-1} h^{-1} [31]. Lower initial catalytic activity is also observed for complexes containing ethylenediamine ligands [16]. The observed specific initial rates for the supported catalysts are superior to those exhibited by other similar systems comprising (chloro)dioxomolybdenum(VI) complexes immobilized in mesoporous materials with surface-bound 1,4-diazabutadiene groups [27,28], bipyridyl groups [26] and nitrile (NCR) groups [25].

The stability of the supported catalysts was further checked by recycling the catalysts twice under identical reaction conditions. After 24 h reaction, the solid was separated from the reaction products by filtration and washed thoroughly with *n*-hexane and finally dried at room temperature overnight. Powder XRD of the used catalysts showed that the hexagonal symmetry was preserved during catalysis. The recovered solids possess similar catalytic performance in recycling runs. Epoxycyclooctane was always the only observed product. Partial loss of activity is observed from the first to the second run but thereafter tends to remains constant (Fig. 4). In the case of MCM-41-PP·MoO_2Cl_2 (**2**), TOF (calculated at 10 min and expressed as mmol g_{cat}^{-1} h^{-1}) follows the order run 1

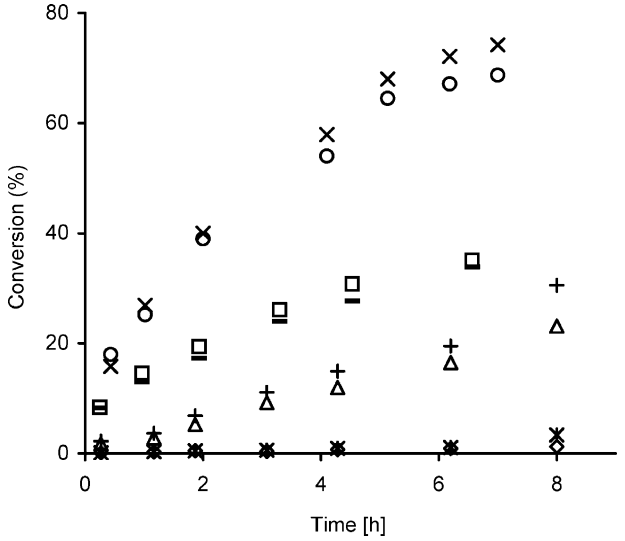

Fig. 5. Kinetic profiles of olefin oxidations with *t*-BuOOH in the presence of MCM-41-PP·MoO_2Cl_2 (**2**) (×; −; *; +) or silylated MCM-41-PP·MoO_2Cl_2 (**4**) (open symbols): α-pinene (−; □); *R*-(+)-limonene (×; ○); 1-octene (*; ◇); *trans*-2-octene (+; Δ).

(268) > run 2 (21) ≈ run 3 (16). Similarly, for silylated MCM-41-PP·MoO_2Cl_2 (**4**), the order is run 1 (277) > run 2 (23) ≈ run 3 (18). These results suggest that changes in the amount and/or chemical nature of the supported molybdenum species may have occurred during the first reaction cycle. Leaching tests were performed for both **2** and **4** by filtering the reaction mixture at the reaction temperature and leaving the solution to react further. In both cases, the reaction proceeds without catalyst but the conversion rate is approximately half that observed in the presence of a catalyst. We may conclude that the first reaction cycle is at least partly catalyzed in homogeneous phase, probably by weakly adsorbed molybdenum species that were not efficiently extracted after the final grafting step in the synthesis of the materials. The amount of molybdenum present in the used catalysts was measured by ICP-AES, which showed a reduction in the metal content of 6% for **2**, but no reduction in the case of **4**. These results indicate that the undesired slight leaching of the catalyst can be inhibited by the postsynthesis trimethylsilylation step, in agreement with results for heterogenized oxodiperoxo molybdenum chelate complexes [22]. IR spectra were measured for the filtered catalysts and also for complex **5** recovered after a catalytic run. The spectra contained the expected Mo=O stretching vibrations, indicating that the formation of oxo-bridged species does not occur or is negligible under the applied oxidizing conditions. For compound **2**, the IR spectrum for the recovered catalyst also contained medium intensity bands at 847 and 2976 cm^{-1}, which indicate the presence of *tert*-butyl groups. The used catalysts may therefore possess some active metal centers coordinated with *tert*-butanol (produced in the consumption of *t*-BuOOH during the first reaction cycle), which could account for the lower initial reaction rates observed. Despite the lower initial rates, after 8 h reaction the conversions approach those achieved in the presence of the fresh catalysts. The retardation effect of *tert*-butanol on the conversion rate of cyclooctene with *t*-BuOOH in the presence of dioxomolybdenum(VI) complexes has been confirmed previously by the addition of this inhibitor at the beginning of the reaction [14].

The catalytic performance of the materials **2** and **4** was further investigated in the oxidation of terpenes, namely α-pinene and (*R*)-(+)-limonene (Fig. 5). The reaction is slower for these substrates than for cyclooctene, under similar reaction conditions, probably due to the higher reactivity of cyclooctene. In the case of α-pinene, selectivity to 2,3-epoxy-pinane is quite low, yielding several other by-products such as campholenic aldehyde, epoxy campholenic aldehyde, myrtenal, 2-pinen-4-one (Fig. 6). The epoxide yield is higher for **4** than for **2**. It is possible that the more hydrophobic surface of the trimethylsilyated material prevents strong adsorption of the epoxide molecules and their subsequent loss in

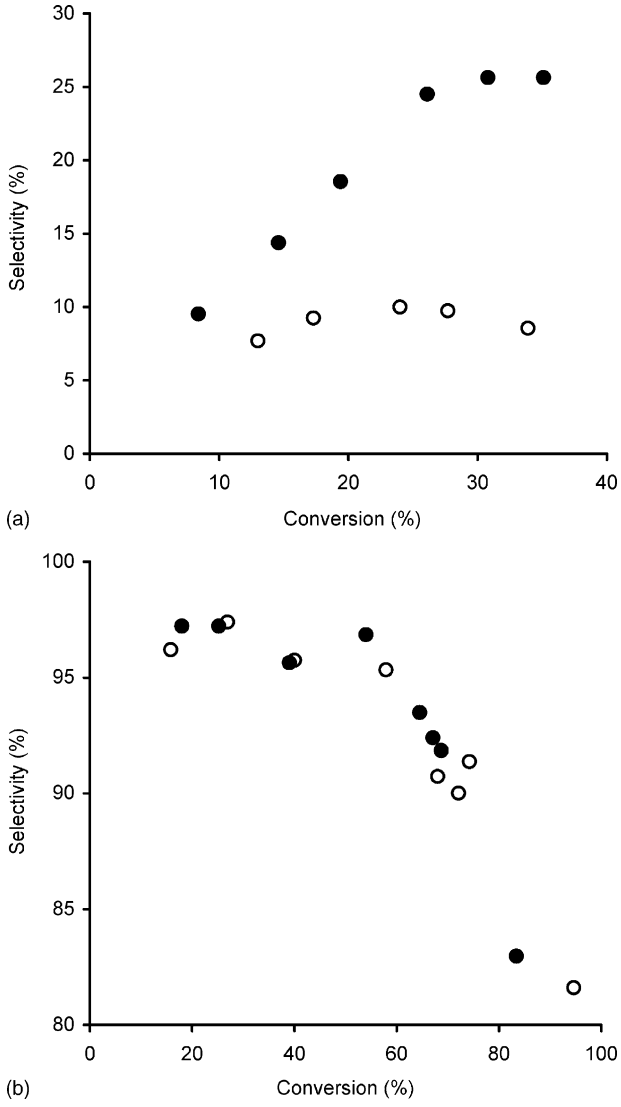

Fig. 6. Selectivity to 2,3-epoxy-pinane (a) and limonene oxide (b) as a function of the conversion of α-pinene (a) and *R*-(+)-limonene (b), respectively, in the presence of MCM-41-PP·MoO_2Cl_2 (**2**) (○) or silylated MCM-41-PP·MoO_2Cl_2 (**4**) (●).

consecutive reactions. The positive influence of trimethylsilylation was also reported by Thiel and co-workers for the epoxidation of cyclooctene in the presence of oxodiperoxo molybdenum chelate complexes covalently anchored onto the surface of mesoporous MCM-41 [21,22]. The catalysts **2** and **4** are particularly attractive for the epoxidation of (*R*)-(+)-limonene, since both yield limonene oxide with high selectivity (>90%) at high conversion (ca. 75%), under relatively mild reaction conditions (328 K, atmospheric pressure, no additional solvent). The 8,9-epoxy-*p*-menth-1-ene and limonene dioxide are the only observed by-products. For less reactive linear olefins, such as 1-octene and *trans*-2-octene, the reaction is much slower than for cyclooctene. Conversions after 8 h decrease in the order cyclooctene (90–93%) < *trans*-2-octene (23–31%) < 1-octene (1–4%). Both catalysts yield the corresponding epoxide as the main product and less than 10% heptanal/hexanal after 24 h reaction with 1-octene/*trans*-2-octene.

4. Conclusions

The inclusion chemistry of MCM-41 functionalized with a pyrazolylpyridine ligand has been further explored using the complex $MoO_2Cl_2(THF)_2$. By using an excess of the precursor complex in the complexation reactions, materials with a molybdenum content of about 0.8 mmol g^{-1} are obtained, which is higher than the ligand content of 0.45 mmol g^{-1}. The spectroscopic data indicate that the surface-bound chelating ligands bind strongly with MoO_2Cl_2 units. As a result, lower metal loadings can easily be achieved by controlling the excess of $MoO_2Cl_2(THF)_2$ used. The supported materials are active and selective for the epoxidation of olefins using *t*-BuOOH as the oxidant. In fact, compared with other materials prepared by us using $MoO_2Cl_2(THF)_2$ and functionalized MCM-41, the catalytic results found in the present work are substantially better. Concerning stability, some activity is lost from the first to second runs, but thereafter the solids can be recycled without significant loss of activity. Tests indicate that the recycled solids operate as true heterogeneous catalysts. The loss in activity from the first to second runs is frequently observed for these types of materials containing heterogenized dioxomolybdenum(VI) complexes. Characterization work of fresh and used catalysts is underway in order to get a better understanding of this phenomenon.

Acknowledgements

The authors are grateful to FCT, OE and FEDER for funding (Project POCI//QUI/56109/2004). We also wish to thank the University of Aveiro and the FCT for research grants (to JAF).

References

[1] W.R. Thiel, M. Angstl, T. Priermeier, Chem. Ber. 127 (1994) 2373.
[2] W.R. Thiel, M. Angstl, N. Hansen, J. Mol. Catal. A: Chem. 103 (1995) 5.
[3] W.R. Thiel, T. Priermeier, Angew. Chem. Int. Ed. Engl. 34 (1995) 1737.
[4] W.R. Thiel, J. Eppinger, Chem. Eur. J. 3 (1997) 696.
[5] F.E. Kühn, A.M. Santos, I.S. Gonçalves, C.C. Romão, A.D. Lopes, Appl. Organomet. Chem. 15 (2001) 43.
[6] R. Clarke, D.J. Cole-Hamilton, J. Chem Soc., Dalton Trans. (1993) 1913.
[7] F.J. Arnaiz, R. Aguado, J.M.M. Ilarduya, Polyhedron 13 (1994) 3257.
[8] M. Miggins, U.K. Kakarla, D.A. Knight, J.C. Fettinger, An. Quim. Int. Ed. 92 (1996) 59.
[9] F.E. Kühn, A.D. Lopes, A.M. Santos, E. Herdtweck, J.J. Haider, C.C. Romão, A.G. Santos, J. Mol. Catal. A: Chem. 151 (2000) 147.
[10] F.E. Kühn, A.M. Santos, A.D. Lopes, I.S. Gonçalves, E. Herdtweck, C.C. Romão, J. Mol. Catal. A: Chem. 164 (2000) 25.
[11] M. Groarke, I.S. Gonçalves, W.A. Herrmann, F.E. Kühn, J. Organomet. Chem. 649 (2002) 108.
[12] F.E. Kühn, M. Groarke, É. Bencze, E. Herdtweck, A. Prazeres, A.M. Santos, M.J. Calhorda, C.C. Romão, I.S. Gonçalves, A.D. Lopes, M. Pillinger, Chem. Eur. J. 8 (2002) 2370.
[13] A.A. Valente, J. Moreira, A.D. Lopes, M. Pillinger, C.D. Nunes, C.C. Romão, F.E. Kühn, I.S. Gonçalves, New J. Chem. 28 (2004) 308.
[14] A. Al-Ajlouni, A.A. Valente, C.D. Nunes, M. Pillinger, A.M. Santos, J. Zhao, C.C. Romão, I.S. Gonçalves, F.E. Kühn, Eur. J. Inorg. Chem. (2005) 1716.
[15] G. Wang, G. Chen, R.L. Luck, Z. Wang, Z. Mu, D.G. Evans, X. Duan, Inorg. Chim. Acta 357 (2004) 3223.
[16] Ž. Petrovski, M. Pillinger, A.A. Valente, I.S. Gonçalves, A. Hazell, C.C. Romão, J. Mol. Catal. A: Chem. 227 (2005) 67.
[17] M.K. Trost, R.G. Bergman, Organometallics 10 (1991) 1172.
[18] M. Abrantes, A.M. Santos, J. Mink, F.E. Kühn, C.C. Romão, Organometallics 22 (2003) 2112.
[19] J. Zhao, A.M. Santos, E. Herdtweck, F.E. Kühn, J. Mol. Catal. A: Chem. 222 (2004) 265.
[20] A.A. Valente, J.D. Seixas, I.S. Gonçalves, M. Abrantes, M. Pillinger, C.C. Romão, Catal. Lett. 101 (2005) 127.
[21] M. Jia, W.R. Thiel, Chem. Commun. (2002) 2392.
[22] M. Jia, A. Seifert, W.R. Thiel, Chem. Mater. 15 (2003) 2174.
[23] M.J. Hinner, M. Grosche, E. Herdtweck, W.R. Thiel, Z. Anorg. Allg. Chem. 629 (2003) 2251.
[24] M. Jia, A. Seifert, M. Berger, H. Giegengack, S. Schulze, W.R. Thiel, Chem. Mater. 16 (2004) 877.
[25] P. Ferreira, I.S. Gonçalves, F.E. Kühn, A.D. Lopes, M.A. Martins, M. Pillinger, A. Pina, J. Rocha, C.C. Romão, A.M. Santos, T.M. Santos, A.A. Valente, Eur. J. Inorg. Chem. (2000) 2263.
[26] C.D. Nunes, A.A. Valente, M. Pillinger, A.C. Fernandes, C.C. Romão, J. Rocha, I.S. Gonçalves, J. Mater. Chem. 12 (2002) 1735.
[27] C.D. Nunes, M. Pillinger, A.A. Valente, J. Rocha, A.D. Lopes, I.S. Gonçalves, Eur. J. Inorg. Chem. (2003) 3870.
[28] C.D. Nunes, M. Pillinger, A.A. Valente, A.D. Lopes, I.S. Gonçalves, Inorg. Chem. Commun. 6 (2003) 1228.
[29] S. Gago, M. Pillinger, A.A. Valente, T.M. Santos, J. Rocha, I.S. Gonçalves, Inorg. Chem. 43 (2004) 5422.
[30] A. Sakthivel, J. Zhao, M. Hanzlik, F.E. Kühn, J. Chem. Soc., Dalton Trans. (2004) 3338.
[31] M. Abrantes, S. Gago, A.A. Valente, M. Pillinger, I.S. Gonçalves, T.M. Santos, J. Rocha, C.C. Romão, Eur. J. Inorg. Chem. (2004) 4914.
[32] A. Sakthivel, J. Zhao, G. Raudaschl-Sieber, M. Hanzlik, A.S.T. Chiang, F.E. Kühn, Appl. Catal. A: Gen. 281 (2005) 267.
[33] A. Sakthivel, J. Zhao, M. Hanzlik, A.S.T. Chiang, W.A. Herrmann, F.E. Kühn, Adv. Synth. Catal. 347 (2005) 473.
[34] C. Li, Catal. Rev. 46 (2004) 419.
[35] M. Kruk, M. Jaroniec, A. Sayari, Langmuir 13 (1997) 6267.
[36] M. Kruk, V. Antochshuk, M. Jaroniec, A. Sayari, J. Phys. Chem. B 103 (1999) 10670.
[37] W.M. Carmichael, D.A. Edwards, G.W.A. Fowles, P.R. Marshall, Inorg. Chim. Acta 1 (1964) 93.
[38] H. Brunner, T. Scheck, Chem. Ber. 125 (1992) 701.
[39] S. Gago, Y. Zhang, A.M. Santos, K. Köhler, F.E. Kühn, J.A. Fernandes, M. Pillinger, A.A. Valente, T.M. Santos, P.J.A. Ribeiro-Claro, I.S. Gonçalves, Micropor. Mesopor. Mater. 76 (2004) 131.

[40] C.D. Nunes, A.A. Valente, M. Pillinger, J. Rocha, I.S. Gonçalves, Chem. Eur. J. 9 (2003) 4380.
[41] Y. Song, Y. Huang, E.A. Havenga, I.S. Butler, Vib. Spectrosc. 27 (2001) 127.
[42] S.J. Gregg, K.S.W. Sing, Adsorption, Surface Area and Porosity, 2nd ed., Academic Press, London, 1982.
[43] M. Kruk, M. Jaroniec, S. Guan, S. Inagaki, J. Phys. Chem. B 105 (2001) 681, and references cited therein.
[44] D. Brunel, A. Cauvel, F. Fajula, F. DiRenzo, in: L. Bonneviot, et al. (Eds.), Zeolites: A Refined Tool for Designing Catalytic Sites, Elsevier Science B.V., 1995, p. 173.